

models of the form

$$\begin{bmatrix} x_0(t+1, k_1, \dots, k_N) \\ x_1(t, k_1+1, \dots, k_N) \\ x_{-1}(t, k_1-1, \dots, k_N) \\ \vdots \\ x_{-n}(t, k_1, \dots, k_N-1) \end{bmatrix} = Ax(t, k_1, \dots, k_N) + Bu, \quad (4)$$

$$x = [x_0^T \ x_1^T \ x_{-1}^T \ \dots \ x_{-n}^T]^T, \quad (5)$$

$$y(t, k_1, \dots, k_N) = Cx(t, k_1, \dots, k_N) + Du, \quad (6)$$

where y , x , x_0 , \dots , x_{-n} , $u = u(t, k_1, \dots, k_N)$ are vector-valued functions and A , B , C , D are constant matrices of appropriate sizes. The system (4)–(6) can be represented as an LFT of a constant matrix with a frequency structure that includes discrete Laplace variables for the spatial coordinates and their inverses. In [8], [9], [10] the stability, closed-loop control design, and other dynamics issues for such multidimensional systems are studied through algebraic properties of the multivariable transfer functions given by the LFT.

For causal systems, including Roesser multidimensional systems (1), the ambiguity between a transfer function and one of its realizations “is benign and convenient and can be always resolved from the context” [31, Section 10.2, p. 257]. Unfortunately this is not the case for non-causal multidimensional systems. First, it is important to note that unlike (1)–(3) the equations (4)–(6) cannot in fact be considered a realization of a non-causal multidimensional system. Some of the update schemes corresponding to an “equivalent” model of the form (4)–(6) can be stable, others unstable in the non-causal coordinates. This is similar to the mathematical theory of PDEs where key issues of existence, uniqueness and well-posedness of solution need to be resolved before analytical techniques, such as ones based on operator transforms, can be used.

Well posedness of a multidimensional system means that its pulse response is absolutely summable along the spatial coordinates. This property is accepted as a basic assumption in [8], [9], [10]. For a system given by equations (4)–(6), these papers assume dealing with a unique well-posed system realization, if such exists. Unfortunately, there are problems with using such approach in control loop analysis. Consider the following simple closed-loop system of the form (4)–(6) with one non-causal coordinate.

$$x(k+1) = u(k), \quad u(k) = ax(k) + w(k), \quad (7)$$

where $w(k)$ is a feedforward input. It is implied in (7) and we assume that the solution x is computed from the input w by performing the update in the causal direction (the direction of increasing index k). This solution can be described by a convolution

$$x(k) = \sum_{n=1}^{\infty} a^n w(k-n) \quad (8)$$

The system (8) is ill-posed (BIBO unstable) for $a > 1$.

The closed-loop transfer function for (7) is $1/(\lambda - a)$, where λ is a discrete Laplace variable corresponding to a unit positive shift operator. Following the approach of [8], [9], [10], for $a > 1$ there is a unique well-posed (BIBO stable) realization

corresponding to the same transfer function. This realization corresponds to the update in (7) being performed in the anti-causal direction and has the form

$$x(k) = \sum_{n=0}^{\infty} a^{-n} w(k+n) \quad (9)$$

Clearly, stability properties and behavior of the system (9) are different from those of system (7) realized as (8). In other words, the stability conditions derived in [8], [9], [10], are necessary, but not sufficient. Some closely related issues for double-sided time axis setups were recently brought to the attention of the control community in [21].

One contribution of this paper is in identifying a large class of practically important multidimensional systems with non-causal coordinates for which closed-loop BIBO stability conditions derived for multidimensional transfer function are also sufficient. The example system (7) does not belong to this class. The key property of systems in this class is that their sampled-time feedback loops do not have direct feedthrough terms (i.e. there is a delay in the causal time coordinate). If this property holds, the closed-loop system will be well posed whenever both the multidimensional plant and the controller are separately well posed. In practice, a sampled-time feedback loop would never have feedthrough terms because of the computation and communication delay inherent in the feedback control. In most practical cases, it can also be established up-front whether the plant and the controller realization are separately spatially stable (well-posed).

The main theoretical contributions of this work are: (i) clarification of robust stability and well-posedness issues for multidimensional systems; (ii) definition of practical analysis approaches for such systems based on an extension of existing μ -analysis tools; and (iii) natural integration of the modeling error caused by boundaries into the analysis framework. The issue of boundary effects was brought up in the recent literature on the subject (e.g., see [10]), but no convenient analysis approach has been proposed so far.

As an example, the proposed multidimensional structured uncertainty analysis (μ -analysis) methodology is applied to closed-loop control of a cross-directional (CD) paper machine process. CD control of paper machines is perhaps the most prominent example of a real-life industrial systems with spatially distributed measurement and control actuation. CD control design and analysis are the subject of many of papers. Most relevant to this work are [25], [26], [27], [13], discussing tuning and analysis of CD controllers with industrially established structures. The example of this paper shows how a structured uncertainty analysis of such closed-loop CD control systems can be carried out in a computationally efficient way while maintaining insight into the process.

The paper is organized as follows: Section 2 provides a formal problem statement and studies well-posedness issues for a general class of multidimensional systems. In Section 3, an approach to Structured Singular Value analysis of such systems is presented. Section 2 and 3 contain the main results of the paper. Section 4 contains an application example of paper machine cross-directional process control.

II. MODELS OF MULTIDIMENSIONAL SYSTEMS

Consider a model of a discrete-time spatially distributed system controlled by an N -dimensional array of actuator and sensor units. Each unit has n control inputs and m measurement outputs. The control, measurement, and dynamical state coordinates of such system can be described as functions of the discrete time t (an integer sample number) and integer spatial coordinates k_1, \dots, k_N (corresponding to the unit number along each of the array dimensions). In a 3-D physical space, an actuator array cannot have more than $N = 3$ dimensions. In the existing applications of array control, $N = 1$ (e.g., linear actuator arrays in paper or printing machines), or $N = 2$ (actively controlled reflectors, other imaging applications).

In what follows, vector or matrix-valued functions $x(t, k_1, \dots, k_N)$ of integer time and spatial coordinates will be considered. The following notations for the norms will be used: $|x|$ will denote a Euclidean norm of a vector or an operator norm (maximal singular value) of a matrix; for a function (multidimensional sequence) $x(t, k_1, \dots, k_N)$ the l_2 norm is denoted $\|x\|_2^2 = \sum_{t=0}^{\infty} \sum_{k_1, \dots, k_N=-\infty}^{\infty} |x(t, k_1, \dots, k_N)|^2$. The multidimensional system in question is assumed to be LTI/LSI. The relationship between the control input $u(t, k_1, \dots, k_N)$ and the measurement output $y(t, k_1, \dots, k_N)$ can be described by a multi-dimensional convolution of the input u with a pulse response $H(t, k_1, \dots, k_N) \in \mathfrak{R}^{m,n}$ of the form

$$y(t, k_1, \dots, k_N) = \sum_{\tau=0}^{\infty} \sum_{q_1, \dots, q_N=-\infty}^{\infty} H(t - \tau, k_1 - q_1, \dots, k_N - q_N) u(\tau, q_1, \dots, q_N), \quad (10)$$

System (10) is stable in the Bounded Input Bounded Output (BIBO) sense if for any input u such that $\|u\|_2 < \infty$ the output y is such that $\|y\|_2 < \infty$. BIBO stability requires the pulse response to be absolutely summable. A transfer function $\hat{H} = \hat{H}(z, \lambda_1, \dots, \lambda_N)$ of the distributed system can be calculated as a multi-dimensional discrete Laplace transform (z-transform) of the pulse response H (10):

$$\hat{H} = \sum_{\tau, k_1, \dots, k_N} H(\tau, k_1, \dots, k_N) z^{-\tau} \lambda_1^{-k_1} \dots \lambda_N^{-k_N}, \quad (11)$$

where $z, \lambda_1, \dots, \lambda_N$ are complex Laplace variables. These variables correspond to unit shift operators in time and along each of the N spatial coordinates respectively. For an absolutely summable response (10), the expansion (11) is guaranteed to converge for any complex numbers $z, \lambda_1, \dots, \lambda_N$ in the domain

$$\mathbf{\Lambda}_{1,1} = \{z, \lambda_1, \dots, \lambda_N \in \mathcal{C} : |z| \geq 1, |\lambda_j| = 1\} \quad (12)$$

The following useful enhancement of the above BIBO stability definition and of the domain (12) will be further used in this paper.

Definition 1: A pulse response (10) has *spatial decay rate* r ($r > 1$) and *dynamical growth rate* α ($\alpha > 0$), if the following series is absolutely summable

$$\sum_{t=0}^{\infty} \sum_{k_1, \dots, k_N=-\infty}^{\infty} |H(t, k_1, \dots, k_N)| \alpha^{-t} r^{(|k_1| + \dots + |k_N|)} < \infty, \quad (13)$$

A pulse response satisfying Definition 1 grows more slowly than α^t in time uniformly in the spatial coordinates, and it decays at least as rapidly as $r^{-|l|}$ in space uniformly in time, where $|l|$ is the 1-norm distance from the response center along the spatial coordinates.

The transfer function expansion (11) for an absolutely summable response with a spatial decay rate r and dynamical growth rate α converges uniformly (is analytic) for any complex numbers $z, \lambda_1, \dots, \lambda_N$ in the domain

$$\mathbf{\Lambda}_{\alpha,r} = \{z, \lambda_1, \dots, \lambda_N \in \mathcal{C} : |z| \geq \alpha; r^{-1} \leq |\lambda_{1, \dots, N}| \leq r; r \geq 1; \alpha > 0\} \quad (14)$$

As discussed in more detail later, the spatial decay rate r allows us to specify an acceptable influence of the boundary conditions. This influence decays exponentially at the rate r with the distance from the boundaries. In what follows, a class of *well-posed* systems will be studied

Definition 2: A system is called well-posed if (13) holds for $r = 1$ and some $\alpha > 0$.

The following fact will be central in establishing our results

Proposition 1: Consider a multidimensional system that is described by difference equations (4)–(6) and is known to be well posed. Consider a formal transfer function of the system $\hat{P}(z, \lambda_1, \dots, \lambda_N)$ obtained as an LFT from (4)–(6) and assume that it is analytic in the set $\mathbf{\Lambda}_{\alpha,r}$ (14), where $r, \alpha \geq 1$. Then the system has a spatial decay rate r and dynamical growth rate α .

Proof. Since the transfer function $\hat{P}(z, \lambda_1, \dots, \lambda_N)$ is analytic in $\mathbf{\Lambda}_{\alpha,r}$, it can be expanded as

$$\hat{P}(z, \lambda_1, \dots, \lambda_N) = \sum_{\tau=1}^{\infty} \sum_{k_1, \dots, k_N=-\infty}^{\infty} P(\tau, k_1, \dots, k_N) z^{-\tau} \lambda_1^{-k_1} \dots \lambda_N^{-k_N}, \quad (15)$$

and the expansion converges uniformly in $\mathbf{\Lambda}_{\alpha,r}$. Now consider the transfer function expansion (11) computed for the system pulse response H . In accordance with the well-posedness assumption, the expansion (11) converges in a subset of $\mathbf{\Lambda}_{\alpha,r}$: for $|z^{-1}| < A^{-1}$ ($A > 0$) and $|\lambda_j| = 1$. The formal transfer function \hat{P} coincides with \hat{H} on this subset. Therefore $H(\tau, k_1, \dots, k_N) = P(\tau, k_1, \dots, k_N)$, the transfer function expansion (11) coincides with (15) and converges in $\mathbf{\Lambda}_{\alpha,r}$. In accordance with Definition 1, this guarantees that the proposition statement is true. QED

Proposition 1 requires us to know that that the system is well-posed as a pre-requisite for the transfer function analysis. Consider some important examples of the systems that satisfy this requirement. In practical applications of multidimensional array control, the plant is usually well-posed and can be modeled to have a spatial decay rate $r > 1$. This is because modeling of an array control system as a multidimensional systems is only justified if the influence of the boundary conditions and cross influence of control inputs is small for remote elements of the array. If the cross influence is large

across the entire array, multidimensional system models should not be used in the first place.

An important class of multidimensional systems consists of systems with distributed localized controllers. In such controllers, computations are distributed over nodes associated with each array cell. At each time sample, control values are computed using current data only from the node itself and past data supplied by a few neighboring cells, i.e., new control values computed at other cells cannot be used. Such controller designs reflect important communication constraints existing in large multidimensional array control systems. It can be shown that distributed localized controllers implemented within the described physical constraint on the inter-cell communication are always well-posed.

Proposition 1 helps to establish necessary and sufficient conditions of well-posedness and BIBO stability for a multidimensional systems consisting of interconnected subsystems. The main types of system interconnections are parallel, cascade, and feedback. Establishing well-posedness of a parallel or cascade interconnection of well-posed subsystems is trivial. The feedback case is considered below. Without a loss of generality, consider a unit feedback loop.

Proposition 2: Consider a closed-loop dynamical system that consists of an well-posed multidimensional plant H with a multidimensional controller G in a feedback configuration. Assume further that the feedback loop GH has no feedthrough, i.e., the loop pulse response $(GH)(0, k_1, \dots, k_N) = G(0, k_1, \dots, k_N) \cdot H(0, k_1, \dots, k_N) = 0$. Under these conditions, the closed-loop system is well posed.

Proof. Since the loop does not have a feedthrough and is well posed (as a cascade connection of well-posed plants), its transfer function can be represented in the form $GH(\cdot) = z^{-1}\hat{L}(\cdot)$, where $\hat{L}(\cdot)$ is analytic for $|z^{-1}| < A^{-1}$ and $|\lambda_j| = 1$. In accordance with the Proposition assumptions, the closed-loop transfer function $\hat{H}_c(z, \lambda_1, \dots, \lambda_N)$ can be represented for $z \rightarrow \infty$, and $|\lambda_j| = 1, j = 1, \dots, N$ as

$$\hat{H}_c = [I + z^{-1}\hat{L}]^{-1}z^{-1}\hat{L} \quad (16)$$

Consider the system on the unit circle $|\lambda_j| = 1, j = 1, \dots, N$. Consider $A_c > 0$ such that $|I + z^{-1}\hat{L}| > 0$, for $|z^{-1}| < A_c^{-1}$. The expansion (16) converges uniformly in $z^{-1}, \lambda_1, \dots, \lambda_N$, for $|z^{-1}| < A_c^{-1}$. This follows from [19, Theorem 2, Section 2.4]. To demonstrate that such A_c exists, note that because of the well-posedness the transfer function expansions are uniformly summable for $|\lambda_j| = 1$ and sufficiently large z . The following bound holds: $|\hat{L}(z, \lambda_1, \dots, \lambda_N)| < C$ for $|z| > A$. Thus, for $|z| > A_c = \max(A, 2C)$ we have $|I + z^{-1}\hat{L}| \geq 1 - A_c^{-1}|C| > 1/2$. Consider the closed-loop pulse response with zero lag. Since the loop has no feedthrough, this response is zero and hence absolutely summable. The spatial transfer function $H_c(z = \infty, \lambda_1, \dots, \lambda_N) = 0$ corresponds to this zero-lag pulse response. Hence, by the argument similar to that used in Proposition 1, the well posedness (BIBO stability) follows from the uniform convergence of the expansion (16) in the domain $|z^{-1}| < A_c^{-1}, |\lambda_j| = 1, j = 1, \dots, N$. QED

The essential meaning of Propositions 1 and 2 is that a closed loop consisting of a multidimensional plant and multidimensional controller is well-posed and stable provided

that (i) both the plant and the controller are well-posed (they may be unstable dynamically); (ii) the cascade connection of the controller and plant does not have a feedthrough term; and (iii) the multidimensional closed-loop transfer function is analytic in the stability domain.

Condition (ii) is not very limiting. All it requires is that the control action at each time sample influences the measurements taken from the plant at the next time sample but not the measurements available at the time of computing the control. This always holds in practice. Condition (ii) defines an important constraint in modeling of multidimensional systems. This constraint must be honored for analysis to be consistent. The systems where Condition (ii) is *not* satisfied might include some where a feedback control loop is inside the computations and no physical plant is a part of the loop. This might in principle happen inside controllers, signal or image processings systems, or mathematical models of spatially distributed control.

III. STRUCTURED SINGULAR VALUE ANALYSIS

This section applies results of the previous section to show how the robust stability analysis of a multidimensional control loop can be performed by extending standard methods of Structured Singular Value analysis (μ -analysis). A possibility of applying existing approaches of μ -analysis to multidimensional systems was mentioned in [31], [10]. This possibility follows immediately from an LFT representation of multidimensional systems discussed in [31], [10]. Compared to this earlier work, the contributions of this paper are as follows: (i) This paper presents a study of the *nominal stability* issues. Nominal stability includes the well-posedness requirement and is analyzed based on the results of the previous section. (ii) A provision is made for a guaranteed spatial decay rate of the system pulse response. This permits us to guarantee limits on boundary effects. (iii) The proposed computations can be implemented using the existing standard Mu-tools software [3] and is convenient to apply practically.

A. LFT models

Consider an LFT model corresponding to pseudo state space difference equations of the form (4)–(6), see [8] for more discussion. The LFT model shown in Figure 1 (left) has frequency structure Λ of the form

$$\Lambda = \text{diag} \{ z^{-1}I_n, \lambda_1 I_{p_1}, \lambda_1^{-1} I_{n_1}, \dots, \lambda_N I_{p_N}, \lambda_N^{-1} I_{n_N} \}, \quad (17)$$

where I_j is a unity matrix of the size j and the dimensions are as appropriate.

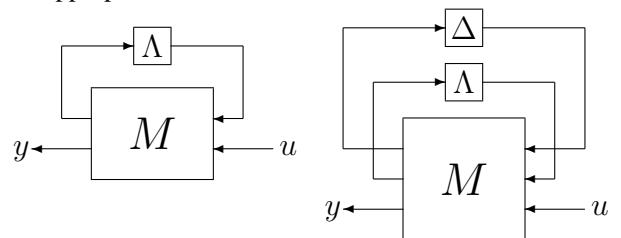


Fig. 1. LFT models

The LFT model in Figure 1 (left) can be extended to take into account model uncertainty $\Delta \in \mathbf{\Delta}$. Here Δ describes a realization of uncertainty, and $\mathbf{\Delta}$ is the uncertainty set. Consider the following uncertainty structure that is as usual in the Structured Singular Value analysis - μ -analysis.

$$\Delta = \text{diag} \left\{ \delta_1 I_{r_1}, \dots, \delta_S I_{r_S}, \delta_{S+1} I_{q_1}, \dots, \delta_{S+Q} I_{q_Q}, \right. \\ \left. \Delta_1, \dots, \Delta_F \right\}, \quad (18)$$

where δ_s are real or complex scalars, and Δ_f are square complex matrix blocks. A more detailed discussion of the uncertainty description (18) and explanation of its physical meaning can be found in the textbook [31]. It what follows, it is assumed that the complex uncertainty Δ corresponds to a transfer function of a well-posed and stable system (see Definition 2).

The LFT model including the uncertainty is shown schematically in Figure 1 (right). The two upper blocks in the feedback loop include the uncertainty description (18) and frequency structure (17). The transfer function (11) with the uncertainties (18) can be presented in the LFT form as

$$\hat{P}(z, \lambda_1, \dots, \lambda_N; \Delta) = M_{22} + M_{21} \bar{\Delta} (I - M_{11} \bar{\Delta})^{-1}, \\ \bar{\Delta} = \text{block diag} \{ \Delta, \Lambda \}, \quad (19)$$

where the submatrices M_{ij} of the matrix M provide a partitioning compatible with (18), (17) and Figure 1 (right). As usual, it is assumed that the uncertainties (18) have been scaled such that they belong to a set

$$\mathbf{\Delta} = \left\{ \delta_1, \dots, \delta_S \in \mathfrak{R}, \delta_{S+1}, \dots, \delta_{S+Q} \in \mathfrak{C}, \Delta_j \in \mathfrak{C}^{m_j, m_j} : \right. \\ \left. |\delta_k| \leq 1, \bar{\sigma}(\Delta_j) \leq 1 \right\} \quad (20)$$

At this point it is important to emphasize that there are some differences in the modeling of multidimensional systems compared to the standard system modeling in μ -analysis of dynamical systems. Unlike standard LFT models, in (17), both spatial Laplace variables λ_k and their inverses are included as separate indeterminants. This is done because non-causal FIR response models require using both positive and negative powers of the spatial Laplace variables.

B. Structured singular value

In what follows, the *Multidimensional (MD) Nominal Stability Conditions* are considered to hold unless stated otherwise. These conditions characterize the system in the absence of uncertainty.

Definition 3 (MD Nominal Stability Conditions): Consider a system with uncertainty described by the transfer function (19). Require that in the absence of uncertainty, e.g., for $\Delta = 0$ the system is stable in time and has spatial decay rate r (see Definition 1).

In what follows, MD Nominal Stability Conditions will always be complemented with a condition on the uncertainty used in the robust analysis. The complex uncertainty Δ in (19) corresponds to a transfer function of an unknown uncertainty system. Require that this system Δ is also stable and has spatial decay rate r .

Consider the inner loop in the right diagram in Figure 1. This inner loop includes the frequency structure Λ (17) and defines a transfer function $M(z, \lambda_1, \dots, \lambda_N)$. The diagram in Figure 1 has a closed loop consisting of the system $M(z, \lambda_1, \dots, \lambda_N)$ and the uncertainty Δ . The frequency dependent structured singular value with respect to the uncertainty Δ can be defined as usual [31]

$$\mu_{\Delta}(M(z, \lambda_1, \dots, \lambda_N)) = \frac{1}{\min \{ \bar{\sigma}(\Delta) : \det[I - M(z, \lambda_1, \dots, \lambda_N) \Delta] = 0, \Delta \in \mathbf{\Delta} \}} \quad (21)$$

where $\mathbf{\Delta}$ is as defined in (20) and $\bar{\sigma}(\Delta)$ is the largest singular value (operator norm) of the block matrix Δ .

The Structured Singular Value (SSV) for the system can be defined as an inverse robust stability margin α_{\max} of the system with respect to the uncertainty Δ (18), where the ‘stability’ is understood as the system being stable in time and having a spatial decay rate r in accordance with Definition 1. The structured singular value can be defined as

$$\mu_{\Delta, \Lambda_{\alpha, r}}(M) = \frac{1}{\alpha_{\max}} = \sup_{\Lambda_{\alpha, r}} \mu_{\Delta}(M(z, \lambda_1, \dots, \lambda_N)), \quad (22)$$

where $\Lambda_{\alpha, r}$ is the set (14). The robust stability condition is then $\mu_{\Delta, \Lambda_{\alpha, r}}(M) \cdot \bar{\sigma}(\Delta) < 1$.

The following formulas give a constructive way for computing the SSV (22)

Proposition 3: Assume that the MD Nominal Stability Conditions hold. Then, the structured singular value (21), (22) can be computed as

$$\mu_{\Delta, \Lambda_{\alpha, r}}(M) = \sup_{\omega, \nu_1, \dots, \nu_N \in [0, 2\pi]} \mu_{\Delta, \alpha, r}(M; \omega, \bar{\nu}) \quad (23) \\ \mu_{\Delta, \alpha, r}(M; \omega, \bar{\nu}) = \min_{\rho_n \in \{r^{-1}, r\}} \mu_{\Delta} \left(M(\alpha^{-1} e^{i\omega}, \rho_1 e^{i\nu_1}, \dots, \rho_N e^{i\nu_N}) \right), \quad (24)$$

where $\bar{\nu} = [\nu_1, \dots, \nu_N]^T$, the minimum is computed over all combinations of the factors ρ_n , $n = 1, \dots, N$, with each factor taking one of the two values r or r^{-1} .

The proof of Proposition 3 is based on the fact that the structured singular value $\mu_{\Delta}(M(z, \lambda_1, \dots, \lambda_N))$ (21), (22) is a subharmonic function of each Laplace variable z , $\lambda_1, \dots, \lambda_N$, see [5]. Consider all the above Laplace variables, except λ_1 fixed and in the domain $\Lambda_{\alpha, r}$ (14). By condition of Proposition 3, $M(z, \lambda_1, \dots, \lambda_N)$ is a regular analytic function of λ_1 inside the domain $r^{-1} \leq |\lambda_1| \leq r$. Hence $\mu_{\Delta}(M(z, \lambda_1, \dots, \lambda_N))$ is a subharmonic function of λ_1 in this domain (see [5]) and, thus, achieves its maximum on the domain boundary, i.e., on the set $|\lambda_1| = \{r, r^{-1}\}$. By repeating this reasoning for each of λ_k and z (23), the conclusion (24) follows immediately. Standard μ -tools software can be used in computing (24). Of course, computation of μ is NP-hard in the number of the uncertainties, the same difficulty that is encountered in computing the usual μ .

Proposition 3 requires establishing the multidimensional nominal stability conditions in the absence of uncertainty. Verification of these conditions can be facilitated by the following fact

Proposition 4: Consider a well-posed multidimensional system, with an LFT representation as in Figure 1 (right), where $\Delta = 0$. Assume that the multidimensional transfer function of the system $M(z, \lambda_1, \dots, \lambda_N)$ is such that $M_\infty(\lambda_1, \dots, \lambda_N) = \lim_{|z| \rightarrow \infty} M(z, \lambda_1, \dots, \lambda_N)$ exists and is an analytic function for $r^{-1} \leq |\lambda_j| \leq r$, $j = 1, \dots, N$.

Then the system is well posed, has dynamical growth rate α and spatial decay rate r provided that

$$\max_{\rho_j = \{1/r, r\}} \sup_{\nu_j \in [0, 2\pi]} \rho(M_\infty(\rho_1 e^{i\nu_1}, \dots, \rho_N e^{i\nu_N})) \leq \alpha, \quad (25)$$

where $\rho(M)$ is the spectral radius of the matrix M and the maximum is computed over all combinations of the factors ρ_n , $n = 1, \dots, N$.

Proof. Represent the system as shown in Figure 1 (right) where

$$\begin{aligned} \Delta &= z^{-1} I_n, \\ \Lambda &= \text{diag} \{ \lambda_1 I_{p_1}, \lambda_1^{-1} I_{n_1}, \dots, \lambda_N I_{p_N}, \lambda_N^{-1} I_{n_N} \}, \end{aligned} \quad (26)$$

Note that the pulse response with the zero time lag corresponds to the spatial transfer function $M_\infty(\lambda_1, \dots, \lambda_N) = M(z = \infty, \lambda_1, \dots, \lambda_N)$. The result of Proposition 4 follows from Proposition 1 and Proposition 3 after noticing that (25) presents computation of the Structured Singular Value similar to (23)–(24) for the uncertainty $\Delta = z^{-1} I_n$. The MD Nominal Stability Conditions in Proposition 3 in this case require that the transfer function $M(z = \infty, \lambda_1, \dots, \lambda_N)$ is analytic for $r^{-1} \leq |\lambda_j| \leq r$, $j = 1, \dots, N$ and the pulse response with zero time lag is summable. The latter follows from the well-posedness of the system. QED.

In analysis of controlled dynamical systems, the SSV is commonly computed on a grid of the dynamical frequencies ω . In computing (23), (24), a multidimensional grid of dynamical and spatial frequencies has to be considered. The μ plots used for description of multivariable dynamical systems, here change into $N + 1$ dimensional μ hyper-surfaces (24). Such representation and computations are acceptable, because in present-day practical applications of array control there are only $N = 1$ or $N = 2$ spatial coordinates. At the same time, computers are presently more than 1000 times faster than 20 years ago when SSV was first introduced and used in computations on one-dimensional frequency grids. In the future, 3-D applications of array control might appear, but by then, perhaps, available computing power will have increased further. One important difficulty with the multidimensional SSV plots will be their visualization and interpretation.

Similar to frequency gridding in standard SSV analysis, multidimensional frequency gridding is a reasonable approach to take in many practical applications. Of course, the performance of multidimensional SSV computation is ultimately limited by the fact that underlying problem is NP-hard. This limits the complexity of uncertainty models that can be practically analyzed. Gridding by itself adds computational complexity that is exponential in the number of dimensions in the multidimensional system. This is in line with the result of [29].

Overall the process of the SSV analysis for an uncertain multidimensional system in the LFT form (19) consists of the

following steps:

Step 1: Verify well-posedness of the system for $\Delta = 0$. In practice this often can be done by presenting the system as an interconnected system and applying Propositions 1 and 2. The well-posedness of each of the interconnected subsystems would follow from physical considerations

Step 2: Present system in the LFT form (19) and use Proposition 4 to verify the MD Nominal Stability Conditions. If the controller and the plant in a closed-loop configuration do not simultaneously have feedthrough, the zero lag closed-loop response can be decomposed into the zero lag responses of the plant and controller. Thus the requirement that the pulse response with zero time lag decays faster than $r^{-|x|}$ in the spatial coordinates can be verified separately for the open-loop plant and controller. The remaining analytic condition (25) can be computed using standard μ -tools software.

Step 3: Perform robust stability test by verifying that $\mu_{\Delta, \Lambda, \alpha, r}(M) < 1$. This can be done by using the frequency gridding formulae (23)–(24) and standard μ -analysis tools.

In multidimensional μ -analysis, Step 2 requires verifying analyticity of a multidimensional transfer function $M_\infty(\lambda_1, \dots, \lambda_N)$ in the complex annulus domain $r^{-1} \leq |\lambda_j| \leq r$, $j = 1, \dots, N$, and $r \geq 1$. Let us discuss this in more detail.

Consider first the case of one spatial variable λ . In this case, $M_\infty(\lambda)$ is a usual rational transfer function of a single variable and its poles can be computed directly by one of the well-known methods. The analyticity of the transfer function in a domain means that none of the poles is in the domain.

For multiple (two or three) spatial variables, an important special case is an FIR plant. Practical identification of distributed plants in many cases yields FIR models, e.g., see [15], [16]. This is because the spatial response decaying in spatial coordinate cannot be distinguished from zero once it decays below the level of the measurement noise or other identification inaccuracies. For an FIR plant, $M_\infty(\lambda_1, \dots, \lambda_N)$ is analytic for any variables $\lambda_1, \dots, \lambda_N$.

For $r = 1$, a Linear Matrix Inequality approach applicable for multiple spatial variables is presented in [8], [9], [10]. A computationally efficient and conceptually clean exact solution of the Step 2 problem for a general case of $r > 1$ is an interesting and challenging problem which we hope would attract attention in the control theory community. Such a solution is beyond the scope of this paper. An approximate solution approach is outlined below for the case of $N = 2$ spatial dimensions. This approximate solution can be extended, in principle, to $N = 3$ (or more) dimensions.

Consider the case of $N = 2$, where $M_\infty(\lambda_1, \lambda_2)$ is an LFT with the frequency structure

$$\Lambda = \text{diag} \{ I_{p,1} \lambda_1, I_{n,1} \lambda_1^{-1}, I_{p,2} \lambda_2, I_{n,2} \lambda_2^{-1} \}.$$

The solution steps are as follows:

- Introduce a large parameter α and replace λ_j^{-1} , $j = \{1, 2\}$ by approximations $\lambda_j^{-1} \approx \alpha / (1 + \lambda_j \alpha)$. For $\alpha \gg r$ this approximation is very accurate in the ring $R_r \equiv \{ \lambda_j \in C : r^{-1} \leq |\lambda_j| \leq r \}$. With this approximation the frequency structure becomes $\Lambda_A = \text{diag} \{ I_{n_1} \lambda_1, I_{n_2} \lambda_2 \}$,

where I_{n_j} , $j = \{1, 2\}$ are unity matrices of the sizes $n_j = n_{p,j} + n_{n,j}$. Thus, the condition of the transfer function analyticity can be presented in the form

$$\det[I - A\Lambda_A] \neq 0, \quad \text{for } \lambda_{1,2} \in R_r, \quad (27)$$

where A is a matrix obtained after representing the transfer function as an LFT with the new frequency structure Λ_A . The LFT structure in (27) is illustrated in Figure 2

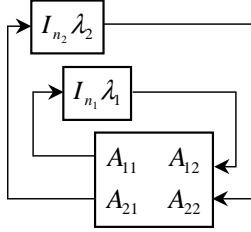


Fig. 2. LFT Representation of the 2-D spatial response transfer function

- Introduce a map $\zeta_2 = \frac{1}{2}(\lambda_2 + \lambda_2^{-1})$. This map transforms the domain $\lambda_2 \in R_r$ into the domain $\zeta_2 \in E_r$, where E_r is the ellipsis

$$E_r \equiv \{\zeta \in C : (\text{Real } \zeta)^2 r^2 + \frac{4(\text{Imag } \zeta)^2}{(r - r^{-1})^2} \leq 1\} \quad (28)$$

Note that each pair of points $\lambda, \lambda^{-1} \in \mathfrak{R}_r$ are mapped onto the same $\zeta \in E_r$. It can be proved that (27) is equivalent to

$$\det[I - 2(A_1^2 + I)^{-1} A_1 \zeta_2] \neq 0, \quad (\lambda_1 \in R_r, \zeta_2 \in E_r), \quad (29)$$

where $A_1 = A_1(\lambda_1)$ corresponds to the LFT including the inner loop in Figure 2 (the loop with λ_1). The expression (29) follows from the fact that $\lambda_2 \in R_r$ iff $\lambda_2^{-1} \in R_r$ and the fact that

$$I - 2(A_1^2 + I)^{-1} A_1 \frac{\lambda_2 + \lambda_2^{-1}}{2} = (A_1^2 + I)^{-1} (A_1 \lambda_2 - I)(A_1 \lambda_2^{-1} - I)$$

An LFT representation of (29) is shown in Figure 3.

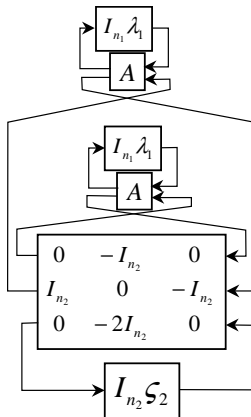


Fig. 3. LFT Representation of the 2-D spatial response transfer function after transforming λ_2 into $\zeta_2 = \frac{1}{2}(\lambda_2 + \lambda_2^{-1})$

Figure 4 shows a representation equivalent to that in Figure 3 and obtained after collecting the indeterminants λ_1 together. The matrix \bar{A} is a block matrix consisting of permutations of the blocks A_{ij} belonging to the two matrices A in Figure 3.

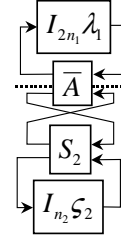


Fig. 4. An equivalent LFT representation of the 2-D spatial response transfer function after transforming λ_2 into $\zeta_2 = \frac{1}{2}(\lambda_2 + \lambda_2^{-1})$

Note that the LFT for the lower part in Figure 4 (below the dotted line) can be represented as $A_2(\zeta_2)$. Similar to how it was done to prove (29), it can be proved that (27) is equivalent to

$$\det[I - 2(A_2(\zeta_2)^2 + I)^{-1} A_2(\zeta_2) \zeta_1] \neq 0, \quad (\zeta_{1,2} \in E_r) \quad (30)$$

An LFT representation of the matrix in the condition (29) is shown in Figure 5.

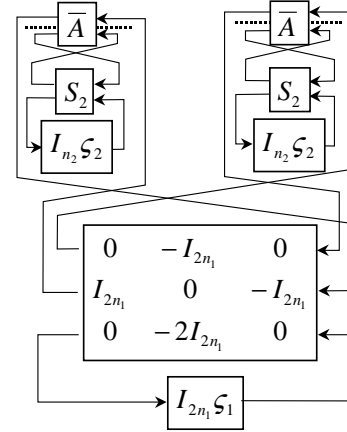


Fig. 5. LFT Representation of the 2-D spatial response transfer function after transforming λ_1 into $\zeta_1 = \frac{1}{2}(\lambda_1 + \lambda_1^{-1})$ and λ_2 into $\zeta_2 = \frac{1}{2}(\lambda_2 + \lambda_2^{-1})$

- Finally, an approximation of the domain (28) can be obtained by substituting $\zeta_j = r^{-1} \delta_j + \frac{1}{2}(r - r^{-1}) \xi_j$, ($j = \{1, 2\}$), where $|\delta_j| \leq 1$ is real uncertainty and $|\xi_j| \leq 1$ is complex uncertainty. By substituting this approximation into the LFT in Figure 5, ‘pulling out’ the indeterminants δ_j and ξ_j the transfer function can be presented in a standard LFT form suitable for standard μ -analysis. Since the domain $\zeta_{1,2} \in E_r$ is a subset of the domain $|\delta_{1,2}| \leq 1, |\xi_{1,2}| \leq 1$, such μ -analysis would give a sufficient condition of the transfer function analyticity.

The above solution steps are described for $N = 2$, but can be extended to $N = 3$. As mentioned earlier, $N > 3$ are not encountered in practical applications.

For modeling and analysis purposes, the summation over an infinite spatial domain is considered in (10). In reality, the spatial domain in question is always bounded, though it may be very large. There is usually a need for considering edge effects that (10) does not address. Edge effects can be proven to be contained in a boundary layer provided the system response taking into account the boundary effects is BIBO stable and decays sufficiently fast in the spatial coordinates. The analysis of the edge effects can be performed by embedding the spatially bounded system into a spatially infinite one. The latter should be setup to match the bounded system inside the bounds to the extent possible. The spatial responses in the system decay exponentially. Therefore, the part of the spatially infinite system solution that is outside of the spatial bounds will influence the solution inside the bounds with an effect that is exponentially vanishing away from the edges. Hence, in general, the spatially infinite model solution will be close to the spatially finite solution except for a boundary layer.

The definition of the structured singular value used in (22) differs somewhat from the standard definition because it includes requirements on the spatial decay rate of the system pulse response. For a given spatial decay rate r the effects of the boundary conditions can be guaranteed to be contained in a boundary layer with a characteristic width $\log r$ near the boundaries of the spatial domain. Through the parameter r , therefore, the impact of the boundary effects can be explicitly included in control design and analysis tradeoffs.

IV. EXAMPLE: CROSS-DIRECTIONAL PROCESS CONTROL

This section demonstrates an application of the analytic approaches described above to a cross-directional process control problem. This is an important industrial application where multidimensional modeling provides adequate tools for practically useful analysis.

A. Motivating industrial application

Paper machines make continuous webs of paper from liquid pulp stock. Paper webs with width up to 10 m go through the machine at speeds up to 100 km/h. Maintaining sufficient uniformity of such critical process variables as paper weight, moisture, and caliper (thickness) across the web width is achieved by using cross-directional (CD) control systems. CD control can include hundreds of spatially distributed actuators influencing the paper process. Measurement systems downstream from the actuators sample the cross-directional profiles of the quality variables and provide feedback errors.

Physics of processes, actuators, and measurements vary greatly in different industrial CD control applications. At the same time, CD process models with the same structure are successfully used in industrial practice for different processes. In the industry, CD process response is commonly modeled as a cascade connection of a dynamical process response and spatial process response. It is usually assumed that the spatial response shapes for all actuators are the same and the responses differ only by corresponding spatial shifts.

A CD control problem can be in principle considered as a standard multivariable control problem, though of very large

size. Structured uncertainty analysis for such systems is briefly surveyed in [6]. Robust analysis in such problems is computationally unfeasible in most cases because the μ -analysis problem is NP-hard and quickly gets out of hand for large plant size [7]. For unstructured uncertainty, significant improvement in computational efficiency of the analysis can be achieved by exploiting the problem structure and performing a modal decomposition of the problem (singular value decomposition of certain spatial operators) [14], [20]. A spatially invariant CD process model can be diagonalized by using the spatial Fourier transform. The papers [25], [26], [27] use such 2-D frequency analysis to deal with an unstructured uncertainty in a CD control problem.

The example of this section demonstrates an application of Section III methodology to a CD control problem. The discussed issues of structured uncertainty analysis and edge effects in CD control have not been addressed in earlier papers. The structured uncertainties correspond to errors in modeling the spatial CD response shape and its center position (actuator mapping). A two-dimensional description of CD control processes without uncertainties was discussed earlier in [18], [30] using Roesser models. Unlike Roesser systems, real-life CD processes are non-causal in the spatial coordinate. The models of this paper are non-causal in the spatial coordinate.

B. Problem Formulation

The CD process variables depend on two integer coordinates: a sampled cross-directional coordinate $x \in Z$ corresponding to an actuator number and sampled time $t \in Z$. CD actuators are numbered by the CD coordinate x . The scalar control variable u is, thus, a function of time and CD coordinate, $u = u(x, t)$. There is a scalar output error variable $y = y(x, t)$.

A paper machine CD process is commonly modeled as a separable process that can be described as a cascade connection of a dynamical response and spatial response subsystems of the form

$$y(x, t) = G(\lambda, \lambda^{-1})g(z^{-1})u(x, t) + \xi(x, t), \quad (31)$$

where $\xi(x, t)$ is an external disturbance acting on the controlled process, z^{-1} is a unit time delay operator and λ^{-1} is a unit left shift operator. In industrial CD process control practice, parametric models of the spatial response and dynamical response are identified from the process data [15], [16]. The spatial operator G in (31) is a two-sided z -transform of the spatial pulse response [22]. A model of spatial response for a CD process is assumed to be of the form:

$$G(\lambda, \lambda^{-1}) = g_0 \Psi(\lambda) \Psi(\lambda^{-1}), \quad (32)$$

$$\Psi(\lambda) = \frac{1}{1 - 2w\zeta\lambda + w^2\lambda^2}, \quad (33)$$

where g_0 is a scalar gain of the process and $\Psi(\lambda)$ is a causal sampled data spatial transfer function. The Wiener-Hopf decomposition (32) allows realization of the non-causal operator $G(\lambda, \lambda^{-1})$ as a composition of causal and anti-causal filters with the transfer functions $\Psi(\lambda^{-1})$ and $\Psi(\lambda)$ respectively.

As commonly assumed in the industry, the dynamical response of the process (31) is a first order response with a unit dead time.

$$g(z^{-1}) = \frac{z^{-1}}{1 - az^{-1}} \quad (34)$$

In the numerical analysis the following values of the process parameters are assumed

$$g_0 = 1, \quad w = 0.55, \quad \zeta = 0.315, \quad a = 0.7 \quad (35)$$

In many CD processes, the general shape of the spatial response is well defined. At the same time, the process gain, location of the response maximum, and response width might differ from the nominal model. This can be well described by a structured (multiplicative) uncertainty replacing (31)

$$y = G(\lambda, \lambda^{-1}) (1 + d_0 \delta(\lambda, \lambda^{-1})) g(z) u + \xi, \quad (36)$$

where δ is an uncertain spatial transfer function, $|\delta(\lambda, \lambda^{-1})| \leq 1$, and the scalar d_0 gives the relative size of the uncertainty. Similar to (31), ξ is the external disturbance.

The analysis for the structured uncertainty model (36) is further compared with the analysis for an unstructured (additive) uncertainty model of the form

$$y = G(\lambda, \lambda^{-1}) g(z) u + g_1 d_0 \delta(\lambda, \lambda^{-1}, z^{-1}) u + \xi, \quad (37)$$

where $|\delta(\lambda, \lambda^{-1}, z^{-1})| \leq 1$ and g_1 is a scalar gain introduced to make the uncertainty scale d_0 in (37) to have the same meaning as in (36).

The control goal is to reduce the influence of the unmeasured disturbance $\xi = \xi(x, t)$ on the process output $y = y(x, t)$. The focus of this example is on the robust *analysis* of a controlled paper machine process. A specific controller structure is assumed herein as commonly used in the industrial CD controllers. The controller is similar to one studied in [25], [26], where more background and explanation can be found. The controller has the form

$$\begin{aligned} \Delta u &= -c(z^{-1})K(\lambda, \lambda^{-1})y - S(\lambda, \lambda^{-1})z^{-1}u, \\ c(z^{-1}) &= k_P(1 - z^{-1}) + k_I, \end{aligned} \quad (38)$$

where $K(\lambda, \lambda^{-1})$ and $S(\lambda, \lambda^{-1})$ are spatial operators and $c(z^{-1})$ is a dynamical PI feedback controller in velocity form. The operator $K(\lambda, \lambda^{-1})$ is chosen to equalize the loop gain across the controllable spatial frequencies while the operator $S(\lambda, \lambda^{-1})$ is chosen to prevent large control action for the poorly controllable modes near the spatial Nyquist frequency. For the numerical example below, these operators are non-causal FIR operators designed using a spatial loopshaping technique similar to [27], [26] as

$$K = k_2 \lambda^{-2} + k_1 \lambda^{-1} + 1 + k_1 \lambda + k_2 \lambda^2 \quad (40)$$

$$S = b_0 + b_1(-0.5 \lambda^{-1} + 1 - 0.5 \lambda) \quad (41)$$

The following controller parameters were assumed

$$\begin{aligned} k_1 = 0.18, \quad k_2 = -0.39, \quad b_1 = 0.005, \quad b_0 = -0.0001, \\ k_P = 0.1, \quad k_I = 0.02, \quad d_0 = 0.5 \end{aligned} \quad (42)$$

C. LFT models for μ -analysis

The structured uncertainty analysis of Section III requires representing the closed-loop CD process (33) with the controller (39) in an LFT form. Following the standard practice [31], the closed-loop multidimensional process (36) with the controller (39) is shown in Figure 6 as an interconnection of simple blocks including the structured uncertainty model in (36). The spatial and dynamical transfer functions g , Ψ , c , K , S in the diagram are defined in (33), (34), (39)–(41). The input of the closed loop system in Figure 6 is the external disturbance ξ . The control performance can be judged by how much this disturbance is suppressed in the system output y .

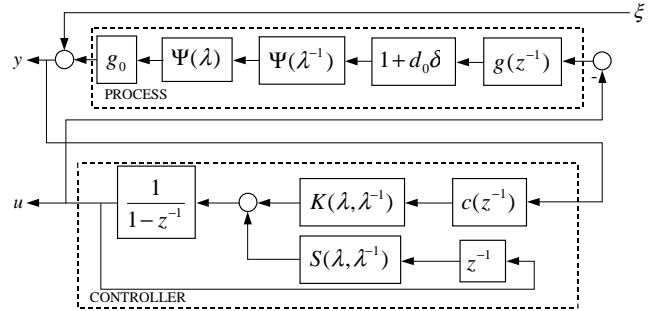


Fig. 6. Closed-loop model of a controlled CD process

The block-diagram model in Figure 6 was used to derive an LFT model shown in Figure 1 (right), where $\Delta = \delta$ is the model uncertainty, and the frequency structure is as follows

$$\Lambda = \text{diag} \{ z^{-1} I_{n_1}, \lambda I_{n_2}, \lambda^{-1} I_{n_3} \}, \quad (43)$$

The dimension parameters are $n_1 = 4$, $n_2 = n_3 = 5$. The matrix M in Figure 1 (right) can be partitioned in accordance with the diagram as $M = \{M_{ij}\}_{i,j=1}^3$.

Consider the requirement of spatial response localization for the closed-loop system. In the numerical example below the spatial decay rate $r = 0.8$ is assumed. This means the response decays by an order of magnitude within 10 steps from its center. The response decay rate defines widths of boundary zones near the edges of the spatial domain of the process. Outside of these boundary zones, the closed-loop system behavior is well approximated by the assumed 2-D model with an infinite spatial domain.

To guarantee dynamical stability and spatial response localization, the multidimensional closed-loop transfer function of the system is required to be analytic in the domain $\Lambda_r = \Lambda_{r,1}$ (14)

$$\Lambda_r = \{z, \lambda \in \mathbb{C} : |z| \geq 1, r \leq |\lambda| \leq r^{-1}, r \leq 1\}, \quad (44)$$

The structured singular value analysis outlined in Subsection III-B begins by verifying the MD Nominal Stability Conditions (see Definition 3). At Step 1, the well posedness of the closed-loop system can be established by applying Proposition 2. The plant (37) and the controller (38)–(41) are each well posed. At Step 2, the condition of the closed-loop zero lag response decaying faster than the chosen rate $r = 0.8$ can be verified separately for the plant and the controller since the latter does not have a feedthrough term. The controller zero

lag response is given by the FIR operator (40). The plant zero lag response is given by (32) and its decay rate can be checked by computing poles of $\Psi(\lambda)$ in (32). Verifying (25) concludes the nominal stability analysis.

The robust stability condition (Step 3 in Subsection III-B) involves the following two-dimensional transfer function from the diagram in Figure 1 (right)

$$M_s(z, \lambda) = M_{11} + M_{12}\Lambda(I - M_{22}\Lambda)^{-1}M_{21}, \quad (45)$$

where M_s is the transfer function between the input to M and output from M associated with δ . The robust stability margin can be defined through a structured singular value μ with the structured uncertainty δ . In accordance with Proposition 3 the structured singular value can be evaluated as (23), (24), where $\alpha = 1$ and $\Lambda_r = \Lambda_{r,1}$ is given by (44). Instead of a usual μ plot, a μ surface $\mu_{\delta,r}(M_s; \omega, \nu)$ is used, where ω is the dynamical frequency and ν is the spatial frequency.

The same LFT model of the closed loop can be used for robust performance analysis very much as described in [31] for dynamical systems. As a performance specification, consider a requirement of the disturbance attenuation: the norm of the transfer function from ξ to y in Figure 1 (right) should be less than d_p , where $d_p < 1$. By pulling out δ , introduce a 2×2 closed-loop multidimensional transfer function $M_p(z, \lambda)$ from ξ and δ to y and δ . Similar to what is discussed in [31], the robust performance requirement can be analyzed by computing the structured singular value similar to (23), (24)

$$\begin{aligned} \mu_{\Delta,1}(M_p; \omega, \nu) &= \mu_{\Delta}(M_p(e^{i\omega}, e^{i\nu})), \\ \Delta &= \text{block diag} \{\delta, \delta_p\}, \end{aligned} \quad (46)$$

where $\delta \in C$ is the process uncertainty (36) and $\delta_p \in C$ is an auxiliary complex uncertainty introduced for the performance analysis. The robust performance requirement holds for all frequencies ω, ν , where $\mu_{\Delta,1}(M_p; \omega, \nu) < 1$.

An important application of the robust performance analysis is in evaluation of the closed-loop bandwidth of the system. A common definition of the control loop bandwidth is as the frequency range, where the external disturbances are attenuated by a factor of $\sqrt{2}$. The bandwidth of the loop subject to the uncertainties can be evaluated by assuming $d_p = 1/\sqrt{2}$ and computing the structured singular value (46). For the two-dimensional process in the question the bandwidth is defined by a two-dimensional domain $B = \{\omega, \nu \in \mathbb{R} : \mu_{\Delta,1}(M_p; \omega, \nu) < 1\}$.

D. Numerical example

Consider now results of the numerical analysis for the closed-loop multidimensional process (36), (33), (34) and the controller (39)–(41) with process parameters (35) and controller parameters (42).

The closed-loop robustness with respect to the complex structured uncertainty δ in (36) is given by the structured singular value $\mu_{\delta,1,r}(M_s; \omega, \nu)$ (24) and is illustrated in Figure 7. One can see that the robust stability is maintained with a large margin.

The structured singular value in Figure 7 can be compared against the robust stability margin with respect to the unstructured additive uncertainty δ in (37). The robust stability margin

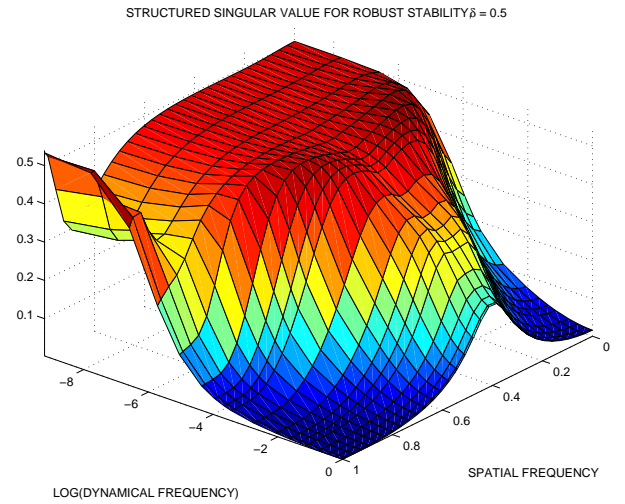


Fig. 7. Generalized μ for robust stability.

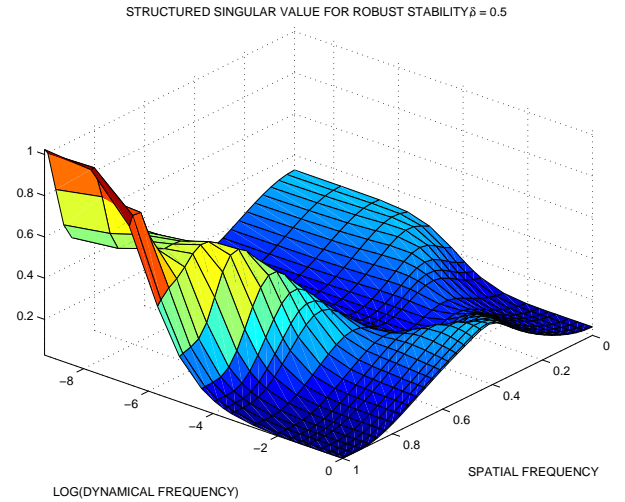


Fig. 8. Unstructured robust stability margin.

obtained from μ -analysis (the same as using the Small Gain Theorem here) and comparable to that in Figure 7 is shown in Figure 8. In this case the maximal singular value $\mu_* = 1.0240$ is almost twice as large as for the structured uncertainty. This means the estimated robustness is twice as bad. This comparison shows that unstructured uncertainty analysis can give overly conservative results for the robustness. The worst deterioration of robustness for unstructured (additive) uncertainty happens near Nyquist spatial frequency. This is because the influence of the structured (multiplicative) uncertainty at this frequency is filtered through the plant transfer function with small gain at this frequency.

Finally, consider the issue of the robust performance and closed-loop bandwidth for the system in question. The structured singular value $\mu_{\Delta,1}(M_p; \omega, \nu)$ (46) that defines the robust performance is plotted in Figure 9. This surface defines bandwidth of the closed-loop system. The closed-loop bandwidth corresponds to the two-dimensional set of the dynamical and spatial frequencies, where the structured singular value in Figure 9 is less than $\sqrt{2}/2$. Figure 10 shows both the robust

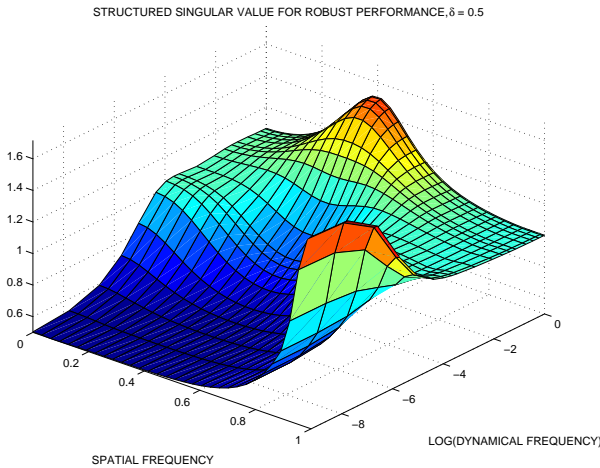


Fig. 9. μ for robust performance

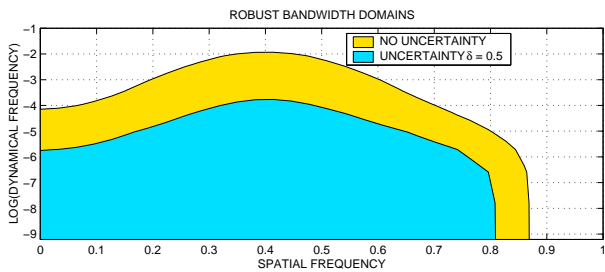


Fig. 10. 2-D bandwidth domains corresponding to robust disturbance attenuation gains of $\sqrt{2}/2$

bandwidth and nominal 2-D bandwidth domain of the closed-loop system. The latter is the bandwidth domain in the absence of the uncertainty, the former is the domain of the guaranteed performance with the structured uncertainty. The presence of the uncertainty shrinks the guaranteed bandwidth, but not too much because of the good robustness of the controller.

V. CONCLUSIONS

The paper presented practical approaches for the analysis of dynamical stability and spatial response localization for linear spatially invariant multidimensional systems. The systems are modeled by multidimensional transfer functions. A Linear Fractional Transformation model for such system can include structured uncertainty. Mathematical analysis of such closed-loop systems has been greatly assisted by that fact that in practice the plant and the controller do not simultaneously have feedthrough terms. The computationally efficient robust stability and localization analysis turns out to be possible via simple extensions of existing μ -analysis tools.

As an example, this paper considered a multidimensional model of a controlled cross-directional (CD) process of web manufacturing. The analysis and modeling approach was illustrated with numerical results representative of paper machine weight control. The analyses were carried out on a modern PC with little computational delay. The established robust stability margins include guarantees on spatial localization of the closed-loop response, that are important in edge effect

analysis, and the robust closed-loop (spatial-dynamical) bandwidth.

REFERENCES

- [1] Bamieh, B., Paganini, F., and Dahleh, M. "Distributed control of spatially-Invariant systems," *IEEE Trans.on Automatic. Contr.*, 2001, to appear.
- [2] Beck, C., Doyle, J., and Glover, K., "Model reduction for multidimensional and uncertain systems," *IEEE Trans. Automat. Contr.*, Vol. 41, No. 10, 1996, pp.1466-1477.
- [3] Balas, G., Doyle, J.C., Glover, K., Packard, A., and Smith R., *μ -Analysis and Synthesis Toolbox*, MUSYN Inc. and The MathWorks Inc., 1991
- [4] Bose, N.K. *Applied Multidimensional Systems Theory*, Van Nostrand Reynhold, 1982
- [5] Boyd, S., Desoer, C.A., "Subharmonic functions and performance bounds on linear time-invariant feedback systems," *IMA Journ. of Math. Control and Information*, vol. 2, 1985, pp. 153–170.
- [6] Braatz, R.D., Ogunnaike B.A., and Featherstone, A.P. "Identification, estimation and control of sheet and film processes," *1996 IFAC World Congress*, San Francisco, CA, pp.319–324, July 1996
- [7] Braatz, R.D., Young, P.M., Doyle, J.C., and Morari, M. "Computational complexity of μ calculation," *IEEE Trans. on Auto. Control*, vol. 39, no. 5, 1994, pp. 1000–1002.
- [8] D'Andrea, R. "Linear matrix inequality approach to decentralized control of distributed parameter systems," *American Control Conf.*, Philadelphia, PA, pp.1350–1354, June 1998
- [9] D'Andrea, R. "Linear matrix inequalities, multidimensional system optimization, and control of spatially distributed systems: An example," *American Control Conf.*, pp.2713-2718, San Diego, June 1999
- [10] D'Andrea, R., and Dullerud, G.E., "Distributed control of spatially interconnected systems," *IEEE Trans. on Automatic Control* (to appear)
- [11] Daniel, M. M., and Willsky, A.S. "Efficient implementations of 2-D noncausal filters," *IEEE Tr. on Circuits and Systems - II: Analog and Digital Signal processing*, vol. 44, no. 7, 1997, pp. 549–563.
- [12] Doyle, J. and Stein, G., "Multivariable feedback design: Concepts for a classical/modern synthesis," *IEEE Trans. Automat. Contr.*, Vol. AC-26, No. 1, 1981, pp. 4-16.
- [13] Duncan, S.R. *The Cross-Directional Control of Web Forming Processes*. PhD thesis, University of London, UK, 1989.
- [14] Duncan, S.R. "The design of robust cross-directional control systems for paper making," *American Control Conf.*, pp. 1800–1805, Seattle, WA, USA, June 1995.
- [15] Gorinevsky, D.M. and Heaven, M. (1997) "Automated identification of actuator mapping in cross-directional control of paper machine," *American Control Conf.*, pp. 3400–3404, Albuquerque, NM, June 1997.
- [16] Gorinevsky, D. and Heaven, M. "Performance-optimized identification of cross-directional control processes," *IEEE Conf. on Decision and Control*, pp. 1872–1877, San-Diego, CA, December 1997.
- [17] Gorinevsky, D., and Stein G., "Structured Uncertainty Analysis of Robust Stability for Spatially Distributed Systems," *IEEE Conference on Decision and Control*, Sydney, Australia, December 2000.
- [18] Heath, W.P., Wellstead, P.E. "Self-tuning prediction and control for two-dimensional processes. Part 1: Fixed parameter algorithms," *Int. J. Control*, vol. 62, No. 1, 1995, pp. 65–107.
- [19] Hurwitz, A., Courant R. *Allgemeine Funktionentheorie und Elliptische Funktionen*, Springer Verlag, Berlin, 1964
- [20] Laughlin, D.L., Morari, M. and Braatz, R.D. "Robust performance of crossdirectional control systems for web processes," *Automatica*, vol. 29, No. 6, 1993, pp. 1395–1410.
- [21] Makila, P.M. "Convolved double trouble," *IEEE Control Systems Magazine*, Vol. 22, No. 4, 2002, pp. 26 -31.
- [22] Oppenheim, A.V., Schaffer, R.W., and Buck, J.R. *Discrete-Time Signal Processing*, Prentice Hall, 1999
- [23] Strikwerda, J.C., *Finite Difference Schemes and Partial Differential Equations*, Wadsworth & Brooks/Cole, 1989
- [24] Roesser, R.P., "A discrete state-space model for linear image processing," *IEEE Tr. on Automatic Control*, vol. AC-20, no. 2, 1975, pp. 1-10.
- [25] Stewart, G., Gorinevsky, D., and Dumont, G. "Design of a practical robust controller for a sampled distributed parameter system," *37th IEEE Conf. on Decision and Control*, pp. 3156–3161, Tampa, FL, December 1998.
- [26] Stewart, G., Gorinevsky, D., and Dumont, G. "Spatial loopshaping: A case study on cross-directional profile control," *American Control Conf.*, pp. 3098–3103, San Diego, CA, 1999.

- [27] Stewart, G., Gorinevsky, D., and Dumont, G. " H_2 loopshaping controller design for spatially distributed systems," *38th IEEE Conf. on Decision and Control*, pp. 203–208, Phoenix, AZ, USA, December 1999.
- [28] Stewart, G., Gorinevsky, D., Dumont, G., Gheorghe, C., and Backstroem J. "The role of model uncertainty in cross-directional control systems," *Control Systems 2000*, pp. 337–345, Victoria, BC, May 2000.
- [29] Toker, O. and Ozbay, H., "On the complexity of purely complex mu computation and related problems in multidimensional systems," *IEEE Trans. on Automatic Control*, Vol. 43, No. 3, pp. 409–414, 1998.
- [30] Wellstead, P.E., Zarrop, M.B., Heath, W.P., et al. "Two-dimensional methods for MD and CD estimation and control: Recent progress," *Pulp and Paper Canada*, vol. 98, No. 9, 1997, pp. T 331–T 335.
- [31] Zhou, K., Doyle, J., and Glover, K., *Robust and Optimal Control*, Prentice Hall, 1996

PLACE
PHOTO
HERE

Dimitry Gorinevsky (M'91–SM'98) is a Senior Staff Scientist with Honeywell Labs (Aerospace Electronics Systems) and a Consulting Professor of Electrical Engineering with Information Systems Laboratory, Stanford University. He received Ph.D. from Moscow Lomonosov University and M.S. from the Moscow Institute of Physics and Technology. He was with the Russian Academy of Sciences in Moscow, an Alexander von Humboldt Fellow in Munich, and with the University of Toronto. Before joining Honeywell Labs he worked on paper

machine control with Honeywell-Measurex and was an Adjunct Professor of Electrical and Computer Engineering at the University of British Columbia, Vancouver, Canada. His interests are in advanced information and control systems applications across many industries. He has authored a book, more than 120 reviewed technical papers and several patents. He is an Associate Editor of IEEE Transactions on Control Systems Technology. He is a recipient of 2002 Control Systems Technology Award of the IEEE Control Systems Society.

PLACE
PHOTO
HERE

Gunter Stein (S'66–M'69–F'85) is a Chief Scientist (ret) of Honeywell Technology Center (now Honeywell Labs). He received a PhD in EE from Purdue University in 1969. His technical specialization is in systems and control, particularly aircraft flight controls (fighters, transports, and experimental vehicles), spacecraft attitude and orbit controls, and navigation systems for strategic, tactical, and commercial applications. From 1977 to 1997, Dr. Stein also served as Adjunct Professor in EE and CS at MIT, teaching control systems theory and design. He is also active

in the development of computer aids for control system design. Dr. Stein was elected fellow of the IEEE in 1985, was awarded the IEEE Control System Society's first Hendrick W. Bode Prize in 1989, was elected to the National Academy of Engineering in 1994, and was awarded the IFAC's Nathaniel Nichols Prize in 1999.